2021 The 21st International Conference on Control, Automation and Systems (ICCAS 2021)
Ramada Plaza Hotel, Jeju, Korea, Oct. 12~15, 2021

The influence of trajectory design parameters on miss distance and survivability of anti-ship missiles

Bui Quoc Dung[1*], Cao Huu Tinh[1], Nguyen Cong Thuc[2], Do Manh Dan[2]

[1] Department of Aerospace Control Systems, Le Quy Don Technical University
Ha Noi, Viet Nam (bqdzung@lqdtu.edu.vn, caohuutinh@lqdtu.edu.vn) * Corresponding author
[2] Naval Academy, Nha Trang, Khanh Hoa, Viet Nam (congthucauto@gmail.com)

Abstract: In this paper, we synthesize the sinusoidal biased proportional navigation guidance (PNG) law for enhancing the survivability of anti-ship missiles against the interception of anti-air missiles (AAM). The magnitude and frequency of the sinusoidal acceleration can be seen as trajectory design parameters of the guidance law. The closed-form solution of the command acceleration is found to show how the key parameters influence the performance of the guidance law. To evaluate the influence of trajectory design parameters as well as dynamics parameters on both the miss distance and the survivability of anti-ship missiles, we use the homing loop model which consists of the canonical fifth-order binomial dynamics and the proposed guidance law. The simulation is implemented in Matlab based on the homing model for drawing the miss distance curves of both anti-ship missiles and anti-air missiles. The simulation results show that the magnitude, frequency, and time constants greatly influence the miss distance and survivability of the anti-ship missiles (ASM). Finally, the suggestions for choosing suitable parameters are also presented.

Keywords: Trajectory design parameters, anti-ship missile guidance, evasive maneuver, survivability, miss distance.

1. INTRODUCTION

The theoretical studies and practical applications have so far shown that the optimal evasive maneuver strategy for evaders is either wavy in the plane or barrel roll in space [4-6]. The studies [7-8] theoretically demonstrated that the optimal evasive maneuver of the ASM will be similar to weaving maneuver in the plane or barrel roll maneuver in the space if there is no information about the anti-air threats. In the work [9] the 3-dimensional biased PNG law has been derived by adding a biased term to the command of PNG law to generate barrel-roll maneuvers. The impact angle control law with sinusoidal evasive maneuver is shown in [10]. The barrel-roll frequency in [9], the magnitude and frequency of the sinusoidal acceleration in [10] can be seen as the trajectory design parameters to shape the maneuver type. The numerical simulations in [9-10] have shown that both the biased PNG law and the impact angle control law can increase the survivability of the ASM against anti-air threats. However, the additional term or the sinusoidal acceleration to the construction of the guidance command can make the miss distance between the ASM and the target ship increase. Therefore, it is necessary to evaluate the influence of the trajectory design parameters on the ASM's miss distance. In addition, the guidance system dynamics used in the simulations of [9-10] are the first-order lag. The disadvantage of this model is that the miss distance can be seriously underestimated [1]. Thus, it is necessary to have a more accurate guidance system model in order to evaluate the perpormance of the guidance law.

In this paper, we first synthesize a guidance law of the ASM to generate weaving maneuvers in the horizontal plane in Section 2. The guidance command consists of a control command term that needs to be figured out to guide the ASM to the target ship and a sinusoidal acceleration term that generates the weaving maneuver. By solving the energy optimal control problem with the terminal constraint, we obtain the sinusoidal biased PNG law. The trajectory design parameters are the magnitude and frequency of the sinusoidal acceleration. In Section 3, we derive a closed-form solution for the ASM's acceleration. The canonical fifth-order binomial homing loop model with the proposed guidance law is presented in Section 4. The simulation analysis of the influence of trajectory design parameters, the parameters of guidance system dynamics, the initial conditions on the ASM's miss distance, and the survivability is shown in Section 5. Finally, the concluding remarks are given in Section 6.

2. GUIDANCE SYNTHESIS FOR EVASIVE MANEUVER OF ANTI-SHIP MISSILES

2.1 Engagement formulation

The problem consists of two entities: an ASM (denoted as M) and a target ship (denoted as T). The $M-T$ engagement geometry in the horizontal plane is depicted in Fig. 1. In this figure, the Ox axis is aligned with the initial line of sight and the Oy is perpendicular to it. We assume that the target ship is stationary and is located at (x_F, y_F). The ASM travels at a constant velocity V_M with a flight-path angle ψ. The ASM's acceleration vector is perpendicular to its velocity vector, denoted as n_M. The range between the ASM and target ship and the line of sight angle are denoted as R_{TM} and λ, respectively. y_{TM} is a relative separation between the

ASM and the target ship.

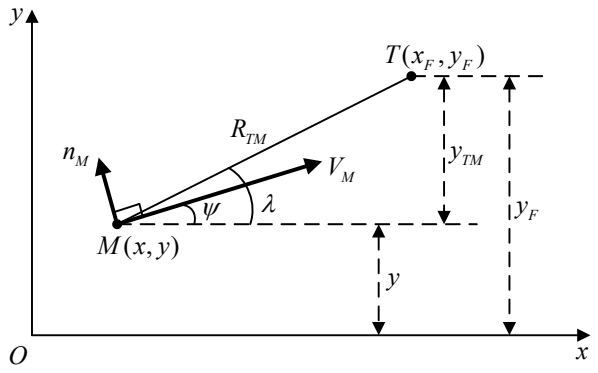

Fig. 1. The engagement geometry between the anti-ship missile and the target ship in the horizontal plane.

From Fig. 1, we can see that if the flight-path angle is small, equations of motion of the missile can be stated as following:

$$\dot{x} = V_M \tag{1}$$

$$\dot{y} = V_M \psi \tag{2}$$

$$\dot{\psi} = n_M / V_M. \tag{3}$$

The command aceleration of the ASM is contructed as following:

$$n_M = n_E + n_C, \tag{4}$$

where n_C is a term that needs to be found to guide the ASM to the target ship, n_E is a sinusoidal acceleration to generate weaving maneuver with a magnitude of k and a frequency of ω. The sinusoidal acceleration can be expressed as follows:

$$n_E = k \sin \omega t. \tag{5}$$

Let $a_S = \sin \omega t$ and $a_C = \cos \omega t$, yields

$$\dot{a}_S = \omega a_C;\ \dot{a}_C = -\omega a_S. \tag{6}$$

The homing time T can be evaluated by integrating both sides of Eq. (1) in the interval time $[0, T]$, yields

$$T = (x_F - x_0) / V_M, \tag{7}$$

where, $x_0 = x(0)$ and $x_F = x(T)$.

The state vector of the ASM – target ship engagement is defined as bellows:

$$\mathbf{x} = [y \quad \psi \quad a_S \quad a_C]^T. \tag{8}$$

The state space equations can be obtain as following:

$$\dot{\mathbf{x}} = \mathbf{A}\mathbf{x} + \mathbf{B}n_C, \tag{9}$$

where

$$\mathbf{A} = \begin{bmatrix} 0 & V_M & 0 & 0 \\ 0 & 0 & \dfrac{k}{V_M} & 0 \\ 0 & 0 & 0 & \omega \\ 0 & 0 & -\omega & 0 \end{bmatrix}, \quad \mathbf{B} = \begin{bmatrix} 0 \\ \dfrac{1}{V_M} \\ 0 \\ 0 \end{bmatrix}. \tag{10}$$

We pose the optimal control problem to find n_C that minimizes the following cost function:

$$J = \frac{1}{2}\int_0^T n_C^2 dt, \tag{11}$$

subject to the system Eq. (9) with the terminal constraint (the miss distance is zero):

$$y(T) = y_F. \tag{12}$$

By solving the optimal control problem, we can obtain an energy optimization guidance law which satisfies the condition is the miss distance is zero. And, it is expected that the guidance law produces the weaving maneuver.

2.2 Synthesis of evasive maneuver guidance law

We use the following transformation [2-3], which can be considered as the new state variable of the system:

$$z(t) = \mathbf{C}\boldsymbol{\Phi}(T,t)\mathbf{x}(t), \tag{13}$$

where $\boldsymbol{\Phi}(T,t)$ is the transition matrix associated with the system, Eq. (9) and satisfying

$$\dot{\boldsymbol{\Phi}}(T,t) = -\boldsymbol{\Phi}(T,t)\mathbf{A},\ \boldsymbol{\Phi}(T,T) = \mathbf{I}, \tag{14}$$

the matrix $\mathbf{C}$ is chosen to satisfy the constraint Eq. (12) as

$$\mathbf{C} = \begin{bmatrix} 1 & 0 & 0 & 0 \end{bmatrix}. \tag{15}$$

Derivating both sides of (13) and using Eqs. (9) and (14), yields

$$\dot{z}(t) = F(t)n_C, \tag{16}$$

where

$$F(t) = \mathbf{C}\boldsymbol{\Phi}(T,t)\mathbf{B}. \tag{17}$$

Because $z(T) = y(T)$, an equivalent reduced-order problem of the preceding optimal control problem is the minimization of the cost function (11) subject to the scalar dynamics and the terminal constraint, Eqs. (16) and (12), respectively.

The Hamiltonian of the problem is

$$H(p, n_C, t) = pF(t)n_C - \frac{1}{2}n_C^2, \tag{18}$$

where $p(t)$ is the co-state variable.

The optimal condition is

$$\frac{\partial H}{\partial n_C} = pF(t) - n_C = 0, \tag{19}$$

yielding

$$n_C = F(t)p. \tag{20}$$

The adjoint equation is

$$\frac{dp}{dt} = -\frac{\partial H}{\partial z} = 0, \tag{21}$$

yielding

$$p = p_0 = const. \tag{22}$$

By using Eqs. (16), (20), and (22), we have:

$$\dot{z} = F^2(t)p_0. \tag{23}$$

Integrating both sides of Eq. (23) in the interval time $[t, T]$, we obtain:

$$z(T) - z(t) = \left[\int_t^T F^2(t)dt\right]p_0. \tag{24}$$

Let

$$G(t) = \int_t^T F^2(t)dt, \tag{25}$$

from Eq (24), yields

$$p_0 = G^{-1}(t)\left[z(T) - z(t)\right]. \tag{26}$$

Using Eqs. (20), (22), and (26), we obtain n_C as follows:

$$n_C = F(t)G^{-1}(t)\left[z(T) - z(t)\right]. \tag{27}$$

Substituting Eq. (27) into Eq. (4), we derive the formula of n_M according to the state vector $\mathbf{x}(t)$ as follows:

$$n_M = \mathbf{M}(t)\mathbf{x}(t) + N(t), \tag{28}$$

where

$$\mathbf{M}(t) = -F(t)G^{-1}(t)\mathbf{C}\boldsymbol{\Phi}(T,t) \tag{29}$$

$$N(t) = F(t)G^{-1}(t)\mathbf{C}\mathbf{x}(T) + ka_S. \tag{30}$$

The state transition matrix $\boldsymbol{\Phi}(T,t)$ is given by the following:

$$\boldsymbol{\Phi}(T,t) = \boldsymbol{\Phi}(T-t) = L^{-1}\left\{(s\mathbf{I} - \mathbf{A})^{-1}\right\}. \tag{31}$$

Let $t_{go} = T - t$ is the time to go, we have

$$\boldsymbol{\Phi}(T,t) = \boldsymbol{\Phi}(t_{go}) = \begin{bmatrix} 1 & \phi_{12} & \phi_{13} & \phi_{14} \\ 0 & 1 & \phi_{23} & \phi_{24} \\ 0 & 0 & \phi_{33} & \phi_{34} \\ 0 & 0 & \phi_{43} & \phi_{44} \end{bmatrix}, \tag{32}$$

where

$$\phi_{12} = V_M t_{go},\ \phi_{13} = \frac{k(1-\cos\omega t_{go})}{\omega^2},$$

$$\phi_{14} = \frac{k(\omega t_{go} - \sin\omega t_{go})}{\omega^2},\ \phi_{23} = \frac{k\sin\omega t_{go}}{\omega V_M},$$

$$\phi_{24} = \frac{k(1-\cos\omega t_{go})}{\omega V_M},\ \phi_{33} = \phi_{44} = \cos\omega t_{go},$$

$$\phi_{34} = -\phi_{43} = \sin\omega t_{go}.$$

From Eq. (17), $F(t_{go})$ is determined as follows:

$$F(t_{go}) = \mathbf{C}\boldsymbol{\Phi}(t_{go})\mathbf{B} = \frac{\phi_{12}}{V_M} = t_{go}. \tag{33}$$

Substituting Eq. (33) into Eq. (25), we obtain $G(t_{go})$ as

$$G(t_{go}) = -\int_{t_{go}}^{0} F^2(t_{go})dt_{go} = \frac{t_{go}^3}{3}. \tag{34}$$

From Eqs. (29) and (30), $\mathbf{M}(t_{go})$ and $N(t_{go})$ are calculated as follows:

$$\mathbf{M}(t_{go}) = -\frac{3}{t_{go}^2}\begin{bmatrix} 1 & \phi_{12} & \phi_{13} & \phi_{14} \end{bmatrix} \tag{35}$$

$$N(t_{go}) = \frac{3}{t_{go}^2}y_F + ka_S. \tag{36}$$

Substituting Eqs. (35) and (36) into Eq. (28), after some algebraic manipulation, yields

$$n_M = \frac{3}{t_{go}^2}[(y_F - y) - V_M\psi t_{go}] + \\ + \frac{\omega^2 t_{go}^2 + 3\cos\omega t_{go} - 3}{\omega^2 t_{go}^2}ka_S + \frac{3\sin\omega t_{go} - 3\omega t_{go}}{\omega^2 t_{go}^2}ka_C. \tag{37}$$

From Fig.1 and $y_{TM} << R_{TM}$, the line of sight angle can be approximated as

$$\lambda = \frac{y_{TM}}{R_{TM}} = \frac{y_F - y}{V_C t_{go}}, \tag{38}$$

where V_C is the closing velocity.

Derivating both sides of Eq. (38) with noting $dt_{go} = -dt$ and using Eq. (2), yields

$$\dot{\lambda} = \frac{(y_F - y) - V_M\psi t_{go}}{V_C t_{go}^2}. \tag{39}$$

Finally, the guidance law is obtained by substituting Eq. (39) into Eq. (37) as follows:

$$n_M = 3V_C\dot{\lambda} + \\ + \frac{\omega^2 t_{go}^2 + 3\cos\omega t_{go} - 3}{\omega^2 t_{go}^2}ka_S + \frac{3\sin\omega t_{go} - 3\omega t_{go}}{\omega^2 t_{go}^2}ka_C. \tag{40}$$

As expected, the synthesized guidance law Eq. (40) is sinusoidal biased PNG law. The command acceleration consists of two terms: the PNG's acceleration which guides the ASM to the target ship and a function of sinusoidal and cosinusoidal acceleration (sinusoidal biased term) that produces the weaving maneuver.

3. CLOSED-FORM SOLUTION

From Fig.1, the relative acceleration can be linearized as follows:

$$\ddot{y}_{TM} = -n_M. \tag{41}$$

Substituting Eq. (40) into Eq. (41) and integrating its both sides, we have:

$$\dot{y}_{TM} = -3V_C\lambda + h(t), \tag{42}$$

where $h(t)$ is the negative part of the integral of the sinusoidal biased term, and after some algebraic manipulations , we obtain:

$$h(t) = \frac{k\cos\omega t}{\omega} - \frac{3k\sin\omega T}{\omega^2(T-t)} + \frac{3k\sin\omega t}{\omega^2(T-t)} + C_1 \tag{43}$$

with C_1 is the constant of integration.

Substituting Eq. (38) into Eq. (42) yields the following first-order time-varying differential equation:

$$\frac{dy_{TM}}{dt} + a(t)y_{TM} = h(t), \tag{44}$$

where

$$a(t) = \frac{3}{T-t}. \tag{45}$$

The Eq. (44) has the following solution [1]:

$$y_{TM} = \exp\left[-\int_0^t a(t)dt\right]\left\{\int_0^t h(t)\exp\left[\int_0^t a(t)dt\right]dt + C_2\right\} \tag{46}$$

where C_2 is the second constant of integration.

C_1 and C_2 can be found by using initial conditions as follows:

$$y_{TM}(0) = 0 \tag{47}$$

$$\dot{y}_{TM}(0) = -V_M HE, \tag{48}$$

where V_M is the ASM's velocity and HE is the heading error in radians.

The closed-form solution for the ASM's acceleration is derived after some algebraic manipulations as follows:

$$n_M = k\sin\omega t + \frac{3k\sin\omega T - 3k\omega T - 3\omega^2 T V_M HE}{\omega^2 T^3}(T-t). \quad (49)$$

This solution will be used as an input of the AAM's homing loop for evaluating the influence of trajectory design parameters on the AAM's miss distance.

4. HOMING LOOP MODEL

The ASM's canonical fifth-order binomial homing loop model with the proposed guidance law is shown in Fig.2.

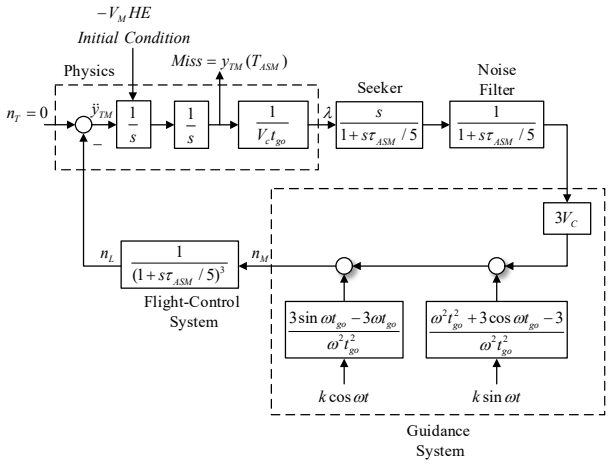

Fig. 2. The ASM's homing loop model

In this homing loop model, we can see that there are three error sources that can produce miss distance: *i)* the initial heading error; *ii)* the sinusoidal and cosinusoidal accelerations characterized by the magnitude k and frequency ω ; *iii)* the dynamics of guidance system characterized by the time constant τ_{ASM} .

Let us consider the engagement between the AAM and the ASM. The AAM has the canonical fifth-order binomial dynamics and uses the PNG law to intercept the ASM which uses the proposed guidance law. The AAM's homing loop model is shown in Fig.3.

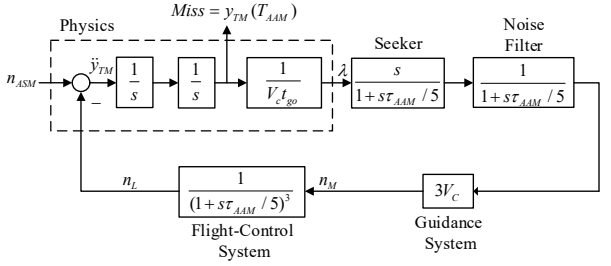

Fig. 3. The AAM's homing loop model

5. SIMULATION ANALYSIS

5.1 Investigating the flight characteristics of the ASM under the application of the proposed guidance law

We simulate the nonlinear engagement between the ASM and the target ship and examine its properties under a variety of circumstances. The simulation conditions are: $(x_0, y_0) = (0,0)$, $(x_F, y_F) = (7000, 0)$, $V_M = 250$ m/s , $k = 5$ g , $\omega = 0.2\pi$ rad/s , $\tau = 0.5$ s , $HE = -20$ deg .

Fig. 4 shows the ASM's trajectories for different frequencies. As expected, those trajectories are the waves and the miss distance is close to zero. We also can see that the ASM's trajectory provided by using the proposed guidance law oscillates around the trajectory given by using the PNG law.

Fig. 5 indicates that the command acceleration oscillates at ω . The maximum value of the command required by the proposed guidance law is much larger than those required by the PNG law.

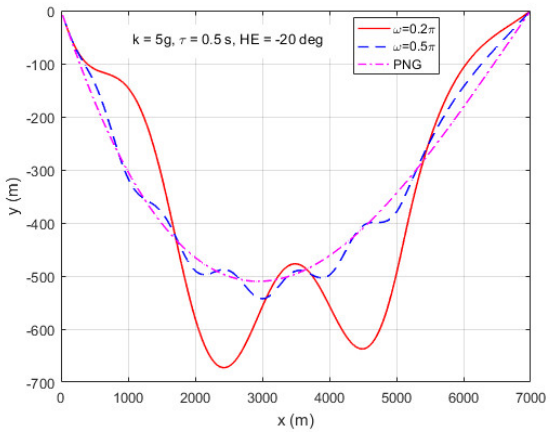

Fig. 4. The ASM's trajectories for different frequencies

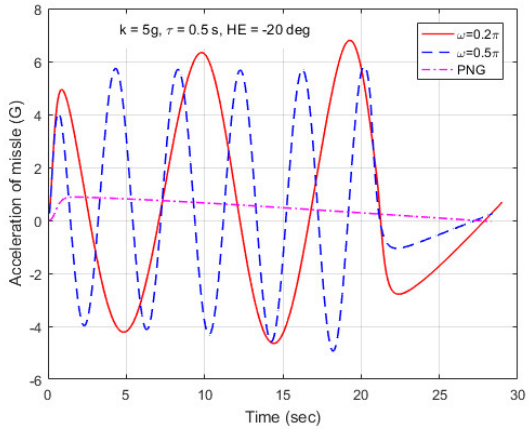

Fig. 5. The ASM's command for different frequencies

5.2 Investigating the influence of trajectory design parameters on the ASM's miss distance.

The simulations are implemented by using the ASM's homing loop model described in Fig.2. Fig. 6 shows the

ASM's miss distance (M.D) for different magnitudes. As can be seen from the figure, a larger magnitude makes an increasing value in the peak of the miss distance. Similarly, the higher the frequency is, the larger the peak of the miss distance is, shown in Fig. 7. In addition, the figure reveals the peak of the miss distance strongly depends on the time constant of the guidance system.

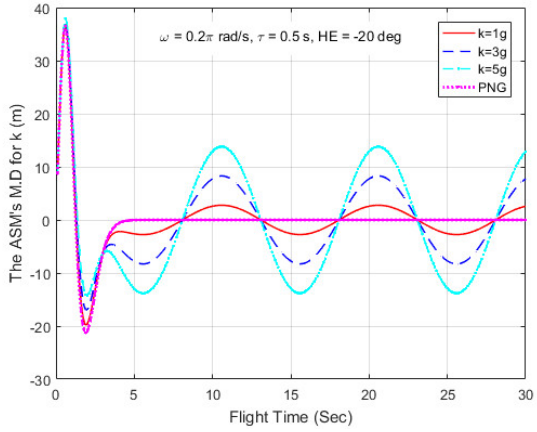

Fig. 6. The ASM's M.D for different magnitude.

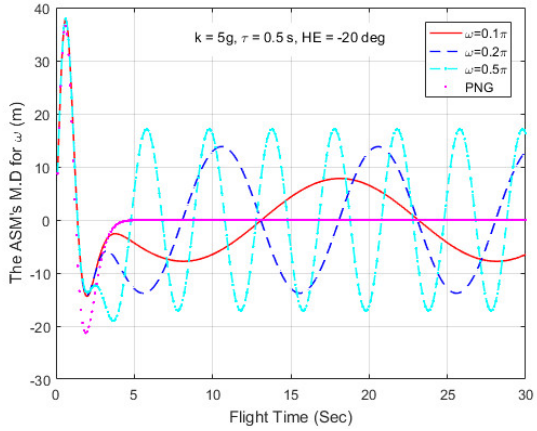

Fig. 7. The ASM's M.D for different frequency.

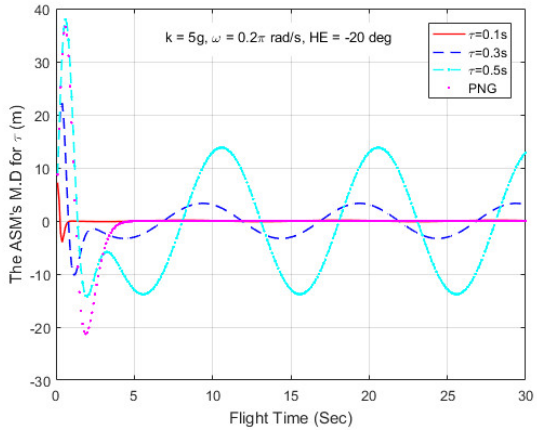

Fig. 8. The ASM's M.D for different time constants.

Fig. 8 indicates that the smaller the time constant is, the smaller the peak of the miss distance is.

Thus, to reduce the ASM's miss distance, we must choose small magnitude and small frequency. However, to generate the best weaving maneuver against the AAM's interception, the proposed guidance law requires a larger magnitude and a right frequency (this will be analyzed in the next simulations). In this case, the time constant is chosen to be small enough to keep the miss distance within the allowable limit. As can be seen from Fig. 8, when the ASM's time constant is 0.1s, the miss distance is almost zero. If the ASM's time constant increases, the miss distance also increases.

5.3 Evaluating the survivability of the ASM with proposed guidance law against AAM's interception

In this section, we examine the survivability of the ASM against interception of the AAM via the AAM's miss distance caused by the ASM's weaving maneuver. The simulations are implemented by using the AAM's homing loop model described in Fig.3.

The fact that the ASM can be intercepted by the AAM at any time during its flight. It is assumed that at a time t_{ASM} (during the ASM's flight), the AAM begins homing to the ASM with a flight time period $T_{AAM} \le T_{ASM} - t_{ASM}$. For each time t_{ASM}, the simulation program is run with different values of T_{AAM}. The ASM's flight time period also has any value within its limit ($T_{ASM} \le T_{ASM}^{\max}$). Thus, we continually run the simulation program with different values of T_{ASM}. Fig. 9 displays the mean of the AAM's miss distance according to the ASM's different flight time period. It is clear that the evasive maneuver of the ASM with the proposed guidance law causes a larger miss distance for the AAM than the PNG law. In other words, there is a higher value in the survivability increases when the ASM performs an evasive maneuver according to the proposed guidance law.

Now, we run all the above programs to obtain the mean of the AAM's miss distance according to the weaving magnitude (k) and weaving frequency (ω_{ASM}) with

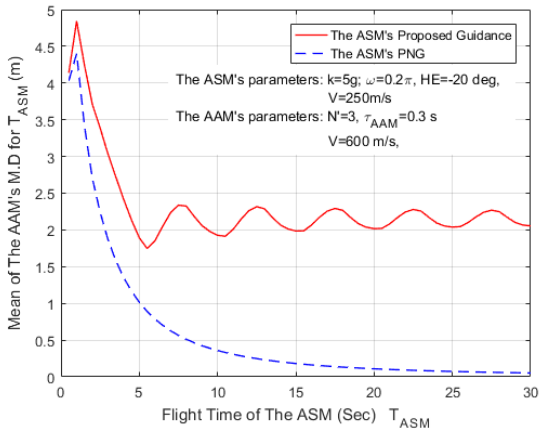

Fig. 9. Mean of the AAM's M.D according to T_{ASM}.

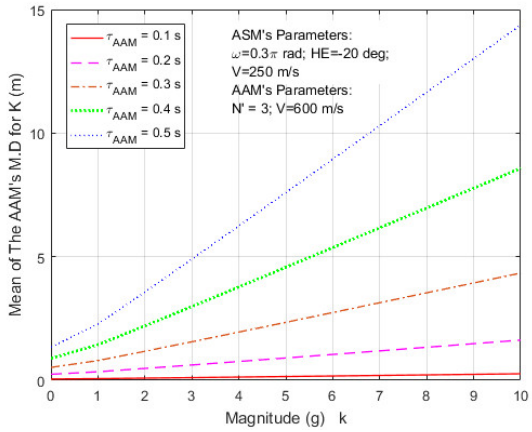

Fig. 10. Mean of the AAM's M.D according to k .

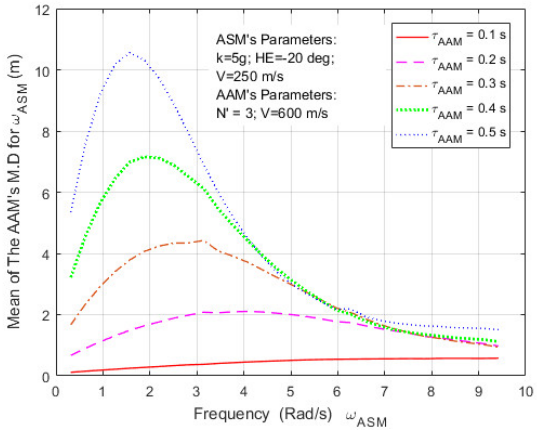

Fig. 11. Mean of the AAM's M.D according to ω_{ASM} .

different AAM's time constants (τ_{AAM}), shown in Fig. 10 and Fig. 11. The simulation results show that the mean of the AAM's M.D always increases when we rise the ASM's weaving magnitude, shown in Fig. 10. Fig. 11 shows that the ASM with both very low and very high weaving frequencies produces a small miss distance for the AAM. In between the two extremes, the mean of the AAM's miss distance increases. From the figure, we also can see that when the product of the AAM's time constant and the ASM's weaving frequency is approximately 0.7, the mean of the AAM's miss distance will reach a maximum. In other words, there exists a frequency such that the ASM's survivability achieves the highest. In addition, it should be noted that the AAM's time constant greatly influences the ASM's survivability. As can be seen from Fig. 11, when the AAM's time constant is equal to 0.1 s, the ASM's survivability is close to zero. The higher the AAM's time constant is, the more up of the ASM's survivability is.

6. CONCLUSIONS

In this paper, we synthesized a sinusoidal biased PNG law. A closed-form solution for the command acceleration of the proposed guidance law was derived, making a crucial contribution when we examine the influence of the trajectory design parameters on the AAM's miss distance, thereby evaluating the ASM's survivability. The simulation results demonstrate that the weaving magnitude and the weaving frequency of the ASM, the time constant of both the ASM and the AAM greatly influence the ASM's survivability and ability to hit the target. The curves of miss distance are meaningful in the preliminary system design. They aid system designers to rapidly predict the performance of a system given a minimum of information. The results also reveal that the guidance system designer must confront in choosing the acceptable guidance system parameters (trajectory design parameters and time constant) to satisfy the trade-offs between the ASM's survivability and its miss distance.

REFERENCES

[1] P. Zarchan, *Tactical and Strategic Missile Guidance*, Sixth Edition, AIAA Progress in Astronautics and Aeronautics, Vol. 239, Inc., Reston, Virginia, 2012.

[2] Bryson, E. A., and Ho, C. Y., *Applied Optimal Control*, Blaisdell, Waltham, MA, 1969.

[3] Gutman, S., *Applied Min-Max Approach to Missile Guidance and Control*, Progress in Astronautics and Aeronautics, Vol. 209, AIAA, Reston, VA, 2005, pp. 232–236.

[4] Shinar J, Rotsztein Y, Bezner E "Analysis of threedimensional optimal evasion with linearized kinematics". *J Guid Control* 2(5):353–360, 1979.

[5] Zarchan P "Proportional navigation and weaving targets," *J Guid Control Dyn* 18(5):969–974, 1995.

[6] Tal Shima "Optimal Cooperative Pursuit and Evasion Strategies Against a Homing Missile," *J Guid Control Dyn* 34(2), 2011.

[7] C. K. Ryoo, I.H. Whang, and M. J. Tahk, "3-D Evasive Maneuver Policy for Anti-Ship Missiles Against Close-In Weapon Systems," AIAA 2003-5653, *AIAA Guidance, Navigation, and Control Conference*, Austin, USA, 2003.

[8] Y. H. Kim, C. K. Ryoo, and M. J. Tahk "Guidance synthesis for evasive maneuver of anti-ship missiles against close-in weapon systems," IEEE Aerosp Electron Syst 46(3):1376–1388, 2010.

[9] Y. H. Kim, C. K. Ryoo and M. J. Tahk, "3-D bias PNG for evasive maneuver of anti-ship missiles against CIWS," *Proceedings of the 16th IFAC Symposium on Automatic Control in Aerospace*, Saint-Petersburg, Russia, 2004, pp.97-102.

[10] J. I. Lee, and C. K. Ryoo, "Impact Angle Control Law with Sinusoidal Evasive Maneuver for Survivability Enhancement," *International Journal of Aeronautical and Space Sciences*, 19(2), 2018.